Chapter 2

Literature review and objectives

2.1 Effect of alloying elements in Fe-Mn-Al-C low-density steels

The Fe-Mn-Al-C alloy system has been increasingly recognized as a promising material for automotive applications over the past several decades. Research indicates that, beyond various thermomechanical processing techniques, the addition of different alloying elements significantly influences the microstructure and tensile properties of these steel. Consequently, the effects of incorporating these alloying elements are examined below:

2.1.1 Effect of manganese

The effect of manganese (Mn) on the tensile properties of Fe-Mn-Al-C steels is related to the aluminium (Al) and carbon (C) content of the steels. Mn stabilizes the austenite phase [49] and forms an almost perfect substitutional solid solution with iron (Fe), displaying almost no solid solution hardening in austenite. Mn can indirectly affect the properties by increasing the volume fraction of austenite as well as the solubility of Al and C in the solid solution. Mn content in the 22–30% range shows similar tensile properties. When the Mn concentration exceeds 30%, it will give rise to β-Mn precipitation, causing extreme brittleness. Hansoo et al. [19] have successfully determined the effect of Mn content on the mechanical properties of Fe-Mn-Al-C alloys, as shown in Fig 4. All the alloys are solution-treated at temperatures above 1000 ℃, followed by water quenching. Additionally, the inclusion of Mn in AHSS contributes significantly to reduce the weight of automobiles without sacrificing strength and ductility. This means that Mn-enhanced steels enable weight reduction in vehicles while maintaining cost-effective production and improved mechanical properties. However, lower Mn content in Fe-Mn-Al-C steels results in reduced formability and ductility, whereas higher Mn content in Fe-Mn-Al-C steels can cause Mn

segregation, leading to poor machinability and corrosion resistance [23]. Therefore, selecting an appropriate Mn content is essential to optimize the tensile and corrosion resistance properties of these steels while keeping production costs reasonable.

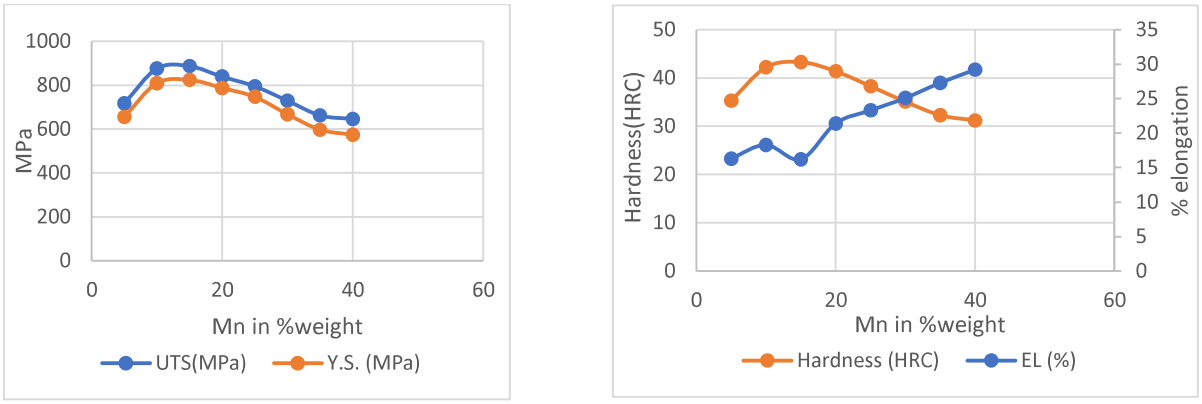

(a) (b)

Fig. 4: The mechanical properties of Fe–10Al–xMn–1.0C alloy sheet castings, (a) the ultimate strength and yield strength, (b) elongation and hardness [13-14, 19, 23, 49].

2.1.2 Effect of aluminium (Al)

The addition of Al to the steels has two important effects besides reducing the density: increasing the stacking fault energy (SFE) and producing κ-carbide [$(Fe, Mn)_3AlC$] precipitates, which affect the mechanical properties and deformation behaviour [50]. For the Fe-30Mn-1.2C-xAl series depicted in Fig. 5a, the alloys depict tensile properties when the Al content is within the 0–9% range after solution treatment. When the Al content exceeds 10%, δ-ferrite begins to form. Compared to the Al-free Fe–30Mn–1.2C TWIP steel, adding up to 7% Al results in a slight increase in yield strength but a decrease in ultimate tensile strength and total elongation. The increase in yield strength is due to the solid solution strengthening effect of Al, while the decrease in ultimate tensile strength is caused by the suppression of mechanical twinning due to the higher SFE. When the Al

content surpasses 8%, yield strength, ultimate tensile strength, and total elongation all increase again, displaying tensile properties similar to the Al-free alloy [11], [14]. This is also confirmed by Raabe et al. [17] that increasing Al content up to 10% increases yield strength, ultimate tensile strength, and TE. However, they also have confirmed that beyond 10% Al, strength increases with severe deterioration of ductility. This is due to the fact that the δ-phase and/or coarse k-carbides are introduced in the austenite grain boundaries, which increase the stress concentration at boundaries. For Fe-30Mn-0.4C-xAl steels (Fig. 5b), the effect of Al on the tensile properties is found to be different. The Fe–30Mn–0.4C steel in as-solutionized condition contains a very small amount of ε-martensite, which leads to a rather low elongation. Another study by Park et al. [50-51] have revealed that in Fe–(20–22)Mn–0.6C–xAl alloys, the microstructure transitions from single-phase austenite to a duplex microstructure consisting of both austenite and ferrite as the Al content exceeds 10%. Notably, the mechanical behaviour of Fe–30Mn–0.9C–xAl alloys shows a consistent trend with that of Fe–20Mn–1.0C–xAl alloys as the Al content varies, despite the significant difference in Mn content.

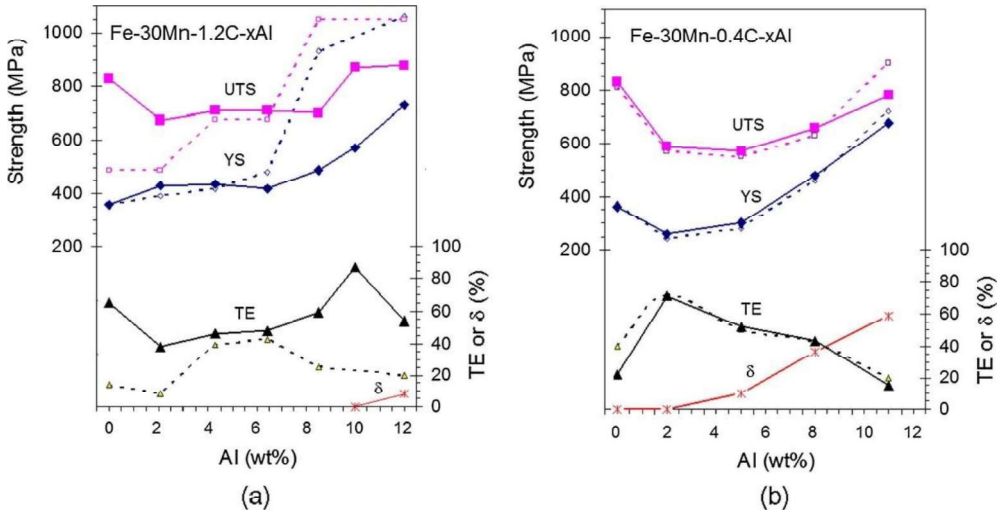

Fig. 5: The tensile properties of (a) Fe-30Mn-1.2C-xAl and (b) Fe-30Mn-0.4C-xAl steels. These steels are subjected to a solution treatment at 1100°C for 2 hours. The solid lines

represent the properties of WQ samples, while the dotted lines correspond to both WQ and aged (at 550°C for 24 hours in an air atmosphere) [11], [14], [17].

So, for the severe deformation processes, the Al content must be in the range of 9% to 10% because, at this weight percentage, the Fe-30Mn-xAl-1.2C steel has the highest elongation which is required during material deformation. Also, the yield strength is below 500 MPa, so the deformation can be produced at a low load supply.

2.1.3 Effect of carbon

The effect of C on the tensile properties of low-density steels is shown in Fig. 6 for steels with two Mn levels. Specimens are solution-treated before oil or water quenching. Figure 6b shows mechanical property changes in Fe-20Mn-10Al-xC alloys [51] which have duplex microstructure at lower C levels. The strength of the alloys increases with increasing C content. Ductility increases to 50 % at 1% carbon content, and then it deteriorates with further carbon content. But in Fig. 6a, Fe-30Mn-9Al-xC [52] alloys show a decrease in strength with the decrease in ductility. Elongation at 1.2% C is about 70%. As the C level is increased, the amount of the austenite increases, and the steels will have a single phase austenite when C reaches a certain level (1% for Fe-30Mn-9Al-xC steels, 1.2% for Fe-20Mn-10Al-xC steels).

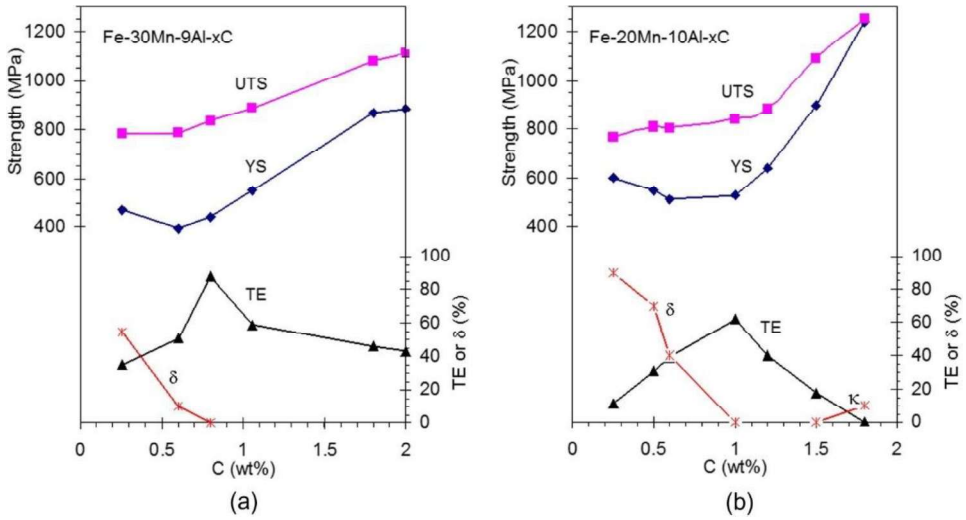

Fig. 6: The tensile properties of (a) Fe-30Mn-9Al-xC and (b) Fe-20Mn-10Al-xC, illustrating the influence of carbon content on their microstructure and tensile properties [51-52].

2.2 Strengthening mechanisms

2.2.1 Solid solution strengthening

The incorporation of solute atoms such as Mn, Al, and Si into the solid solution of the melt significantly enhances the strength of steel compared to pure iron. There are two main types of solid solutions: substitutional and interstitial. In a substitutional solid solution, solute atoms replace solvent atoms in the crystal lattice when they are of similar size. In an interstitial solid solution, smaller solute atoms fit into the spaces or interstices between the larger solvent atoms. For instance, carbon, nitrogen, and boron typically form interstitial solid solutions in steels. The strengthening effect due to solid solution formation is commonly explained in Eq. (1), where σ_{ss} denotes the strengthening component from the solute atoms, which can generally be expressed as [15], [53]:

$$\sigma_{ss} = \sum K_i C_i^{2/3} \quad (1)$$

Where i =1,2,3 for manganese, aluminium, and carbon, respectively. Here, the coefficient K_1 = 2.8, K_2 = 0.8, and K_3 = 187. C_i is the concentration in mass percentage for the i^{th} element.

2.2.2 Grain boundary strengthening

To achieve higher strength, a fine grain size is often necessary in polycrystalline materials. Grain boundaries inherently contribute to material strength, as the interference of slip within the grains enhances this property. Hall introduced a general relationship between yield strength and grain size (Eq. (2)), which was later refined by Petch [15]:

$$\Delta\sigma_g = k\,(g^{-1/2})$$

(2)

Where, k is a material constant, g is the initial grain size. The equation effectively describes how grain size influences flow stress at any level of plastic strain, as well as the extent of ductile or brittle fracture and fatigue strength. In addition to grain boundaries, this equation is also applicable to ferrite-cementite boundaries in pearlite, mechanical twins, and martensitic plates.

2.2.3 Dislocation density strengthening

The yield strength of Fe-Mn-Al-C low-density steel can be significantly enhanced by inducing plasticity and applying SPD through metastable phase transformation. This type of steel, known for its high ductility and relatively low yield strength, has low SFE. This low energy causes dislocations to split into two Shockley partial dislocations, which require stress to recombine into a perfect dislocation capable of moving through the slip plane [54]. This mechanism results in a high strain hardening rate. Strain hardening in Fe-Mn-Al-C steel is achieved through the obstruction of dislocation movement and the interaction of dislocations with the martensite phase that forms during SPD.

2.2.4 Precipitate strengthening

These phenomena result from the formation of fine precipitates, particularly carbides, nitrides, and carbonitrides of various elements. Precipitation hardening involves heat treating and quenching the alloy, during which the second phase, soluble at higher temperatures, precipitates upon quenching and ageing at lower temperatures due to its decreasing solubility. This process enhances the yield strength and ultimate tensile strength of the alloy through the strengthening effect of these fine particles.

2.3 Severe plastic deformation

P.W. Bridges first developed the SPD technique in 1964, motivated by an interest in involving a very large plastic strain for processed material under a hydrostatic state of stress and a shear state of stress for producing bulk ultrafine-grained metallic materials. Fig. 7 below shows the most common SPD method utilized for grain refinement.

Using the HPT method, grain sizes of less than 100 nm can be achieved through the application of extremely high effective strain (3.62) in one pass [55-56]. This technique is particularly effective for significantly deforming relatively brittle or high-strength materials. However, a major drawback of the HPT method is its limitation to small-scale (laboratory) applications, rendering it unsuitable for mass production. Additionally, it often results in inhomogeneous material properties in the central region.

In the ARB process, two strips of metal are bonded together under high load and pressure by passing them through rollers. After each pass through the rollers, the final thickness of the bonded strips remains the same, which allows the process to be repeated multiple times to achieve significant grain refinement (up to 1 μm) and improve the material's mechanical properties [57-58]. Despite the simplicity and effectiveness of this deforming process, it occasionally fails to achieve a uniform bond between the two metal strips. This lack of

uniform bonding can result in inhomogeneous mechanical properties and potential weak spots in the final material.

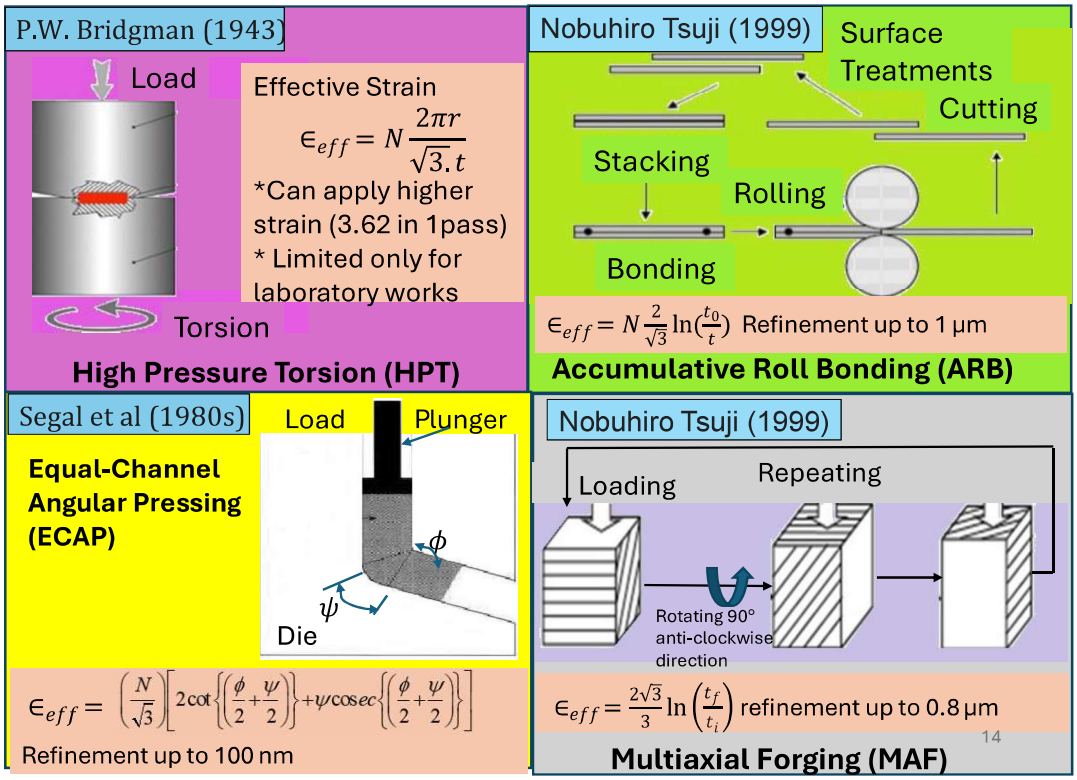

Fig. 7: Different SPD techniques [55-58].

ECAP is a highly effective method for controlling both the microstructure and texture of materials. ECAP is particularly valued for its ability to produce ultrafine grain sizes (up to 100 nm), leading to significant improvements in the material's mechanical properties [59]. Despite recent progress in the field, several challenges remain unresolved. Achieving homogeneous ultrafine grain sizes, especially below the nanoscale, is particularly difficult for very hard materials and large-sized workpieces. Issues such as non-uniform deformation, variations in strain distribution, and maintaining consistent processing conditions across the entire material can lead to inhomogeneities in grain size and

mechanical properties [37]. These challenges highlight the need for further research and development to optimize ECAP processes for a wider range of materials and applications. MAF is one of the SPD techniques that applies force to a metal workpiece along multiple axes to produce refined microstructure to get improved mechanical properties such as higher strength, toughness, and wear resistance [34], [40], [60].

2.3.1 Multiaxial forging

According to the literature, the finest grain size achieved in IF and low carbon steels using the ECAP technique is approximately 0.3 μm and 0.2 μm, respectively. These results were obtained under high equivalent strains of 24 for IF steel and 17 for low C steel. The highest reported yield strength for IF and low carbon steels are 895 MPa and 913 MPa, respectively, accompanied by ductility of 11% and 10.6% [61-62]. However, these techniques often require expensive tooling and present significant design challenges. Additionally, producing bulk samples with uniform ultrafine grain microstructures is difficult with some of these methods [26], [63]. Cold rolling is a deformation technique used to achieve uniform grain refinement and improve strength and wear resistance. However, the degree of refinement is generally limited to 5-10 μm, with strength ranging between 1000-1500 MPa. While cold rolling at room temperature can produce ultrafine grains with strengths exceeding 1500 MPa, it also increases the material's susceptibility to surface cracking. MAF endows excellent ductility among other SPD techniques [39]. While most of the other SPD techniques are typically restricted to laboratory experiments, MAF has proven its advantage in producing bulk refined material for the automotive industry without changing the shape and size of the processed material [30], [34-38]. Some examples of the mechanical properties of ultrafine-grained stainless steel after large deformation are listed in Table 2.

Table 2: Grain size and strength of some ultrafine-grained stainless steels after large deformation.

Processing	Material	Grain size (nm)	Yield strength (MPa)	Ultimate Strength (MPa)	Total Elongation (MPa)	Ref.
HPT at 673 K	SS316	90	1720	1950	8	[64]
HPT at room temperature	SS316	40	1700	1800	7	[64]
HPT at room temperature	S304H	23	1890	1950	17	[65]
ECAP (ε= 8) at 773 K	SS304	80-100	1130	1160	8	[66]
ECAP (ε = 8) at 773 K + annealing at 973 K	SS304	100-150	1045	1115	26	[66]
Rolling at 473 K	SS316L	150	1240	1359	9	[67]
Rolling at 473 K	SS304L	130	1350	1480	8	[67]
Rolling at room temperature	S304H	50	2050	2065	5	[68]
Rolling at room temperature	S316L	70-80	1680	1830	5	[69]

MAF is a method used to significantly enhance the strength of lightweight materials, achieving levels of strength unattainable through other thermo-mechanical processing techniques. It is one of the most effective and straightforward methods for inducing large strains without altering the shape of bulk materials. A key aspect of the MAF technique is volume constancy, which means that by repeating the operation multiple times, the desired grain size can be achieved [37], [59], [70]. This process leads to improvement in mechanical properties such as strength, toughness, hardness, and wear resistance by refining the grains of the material. Close die walls in MAF limit the flow of plastic material and place the specimen under triaxial stress, which causes a simple shear to produce ultrafine-grained materials [71]. This has notable implications for industries, offering

means of property enhancement without necessitating the incorporation of expensive alloying elements. Although, it is a complicated 3-D forging process with unstable and non-uniform plastic deformation, it has been used to improve the mechanical properties after multiple MAF passes of various materials, including copper, magnesium, aluminium, steel alloys, and titanium alloys [38-41].

2.3.2 Grain refinement during multiaxial forging

A typical grain refinement mechanism proceeds with a dynamic recrystallization process and a twin fragmentation mechanism. The domination of either one depends on the flow stress direction, commutative stain, and forming temperature [72].

Muszka et al. [73-74] conducted MAF on IF and HSLA steel, achieving a total strain of approximately 20 with an average grain size of 0.3 μm. The observed increase in strength and hardness is attributed to beneficial structural changes in the material. Similarly, Petryk et al. [75] reported grain refinement to around 0.2 μm in IF steel at a deformation strain of approximately 12 using the same MAF technique. Jie Huang and Zhou Xu [76] have confirmed refined austenite grains in Fe- 32% Ni alloy after MAF. Through SEM images, they have observed that the deformed austenite grains reach 10 μm from the initial 200 μm in 3 passes (1 cycle) and on subsequent passes, it reaches 3~4 μm. The important grain refinement process during MAF is that the initial austenite grain is subdivided gradually into sub-grains by deformed bands [33]. Plastic deformations in MAF are expected to have local fluctuation in crystal orientation within grains in the form of a high dislocation band called a shear band [33], [41]. Even a small loading strain is sufficient to introduce a high number of dense microshear bands (MSBs). When the loading axis is changed, these MSBs interact and form relatively smaller sub-boundaries. Many of these different oriented bands become parallel in the first pass of forging, and in subsequent passes, they interact and cross each other. Due to this, more dislocations accumulate at the boundaries, which lead to an

increase in sub-boundary misorientations. The induced sub-grains are initially enclosed by newly independent low-angle boundaries and later transformed into high-angle boundaries at larger strain, leading to substructure development within the initial grains. MAF provides feasibility in selecting a different set of strain paths during each deformation cycle and gives a proper condition to monitor internal microstructural changes and flow behaviour on subsequent compression. Based on the studies mentioned, it can be concluded that grain size refinement is a crucial technique for enhancing mechanical strength while maintaining ductility.

The activation of deformation twins is also traced within the deformed microstructures simultaneously, the fraction of which increases by increasing imposed strain. At the end of the first pass, the grains are effectively subdivided by multi-variant deformation twins [59]. Miura et al. [77] and N. R. Tao et al. [78] have observed during the grain refining process, and the mechanical twins induce ultrafine-grained structures. Because of coarse grain subdivision by the formation of a high density of mechanical micro twins, these micro twins are further subdivided by dislocation into equiaxed nanocrystalline and lead to the development of nano-grained microstructure by the interaction of dislocations and micro twins.

The grains are also subdivided by martensitic transformation, as observed by Y. Nakao and H. Miura [79]. The strain-induced martensite appears more easily and frequently with increasing strain and/or decreasing deformation temperature in austenitic stainless steels. It is, therefore, suggested that grain refinement in certain materials can be enhanced by a synergetic mechanism involving cDRX, mechanical twinning, and martensitic transformation.

The above literature review demonstrates that the MAF technique induces grain refinement in both ferrous and non-ferrous metals. However, further research is needed on metals

processed using MAF, especially considering the altered strain path associated with this SPD process, making it a compelling study area. Austenitic Fe-Mn-Al-C steels are widely used for structural applications where high strength and good ductility are crucial. MAF processing of austenitic Fe-Mn-Al-C steels is expected to create an ultrafine grain microstructure, enhancing mechanical properties and potentially reducing the reliance on costly alloying elements.

2.3.3 Investigation of deformation behavior

Microstructural development solely depends upon the dislocation's arrangement of various configurations, such as dense dislocation walls on specific slip planes, dislocation tangles, and dislocation cells. Dislocation interactions lead to the formation of sub-grain boundaries across which small misorientations are created.

It is worth mentioning that the previous works regarding the deformation behaviour of TWIP steels through cold rolling [70], [80], HPT [55-56] and friction stir process [81] report the suppression of twinning at the early stage of processing. According to the previous research, the deformation twinning would be suppressed at a 60% reduction during rolling, and the further strains are accommodated by shear bands without any contribution of twinning and slip [82-83]. The deformation mechanism in SPD processes such as HPT is quite different from rolling conditions. The deformation twinning is suppressed at 1/4 turn of the first pass. All the above-mentioned works have been conducted through one deformation path. Deformation twins are suppressed at the early stages with no chance of progressive dislocation slip contribution.

Deformation in austenitic low-density steel occurs by slip, twinning or martensitic transformation, and the choice of method will depend on a significant material parameter called SFE. The deformation of austenite-based lightweight steels is mainly dominated by planar glide due to the high SFE, over 70 mJ/m^2, and dislocations cutting the κ-carbides

[84-85]. In metals with a low value of SFE, the difficulty of cross slip reduces the ability of the material to change its shape during plastic deformation by slip alone, and therefore, deformation twinning may occur. The martensitic transformation takes part in the grain refinement mechanism when mechanical work is done at a lower temperature. Strain-induced martensitic transformation is known to be dominant when the SFE of austenite is less than about 20 mJ/m^2. In metals like austenitic stainless steels with low values SFE of about 20 mJ/m^2, the dislocations dissociate to form stacking faults, and twinning is the preferred mode of deformation. The tendency to deform by twinning is increased if the deformation temperature is lowered or the strain rate is increased.

During forging in all directions, a complex state of stress is induced in the grains. It puts emphasis on the significant influence of the change in strain path on the capability of coupling the deformation twinning with substructure development during room temperature deformation. An interesting grain fragmentation process in austenitic steel has been proposed by Wang et al. [85] during a single compression cycle of MAF. It is suggested that recrystallization behaviour probably takes place during the present interrupted deformation. Therefore, such flow behaviour is associated with progressive strengthening by MAF, and the microstructure changes that take place in the deformed samples should be affected by strain accumulation [86].

2.3.4 Mechanical properties during multiaxial forging

Low strength and ductile austenitic steels are deformed by MAF at temperatures close to the recrystallization (at 700°C) to get an ultrafine grain structure of grain size ~360 nm, which enhances yield strength from ~280 MPa to 730 MPa with high dislocation density of $1.5 \times 10^{15}/m^2$ and ductility of 23% [41-42].

Reducing the deformation temperature to room temperature, MAF of SUS316SS at an equivalent strain of 2.4 increases yield strength from 250 MPa to 1.7 GPa with low ductility

of ~ 10% due to higher refinement, mechanical twinning, and formation of martensite. Further, when imposing equivalent strain up to 6, yield strength increases marginally by about 0.3 GPa, with ductility remaining almost the same [43]. Kim et al. have observed that in MAF (at room temperature) of IF steel, there is continuous improvement in strength with the imposition of increased equivalent strain; even though rate of enhancement decreases at higher strain, ductility is almost unchanged [44]. Rajput et al. performed MAF on 316L stainless steel and found that after the 9th pass, the ultimate tensile strength significantly increased from 506 MPa to 1060 MPa. The Vickers hardness also rose from 230 VHN to 434 VHN, attributed to the buildup of residual stresses with increasing strain. However, this process led to a reduction in toughness, from 3596 mJ/m^3 to 1441 mJ/m^3, and a substantial decrease in elongation, from 74% in the as-received condition to just 8% after the 9^{th} pass [86]. The independence of ductility to imposed strain is primarily brought on by minor changes in the average geometrically necessary dislocation density due to dynamic recovery at higher strain. The MAF process can potentially improve the strength of the material by promoting the emergence of a finer grain structure and higher strain hardening when it is carried out at lower temperatures, but ductility decreases. Ductility increases with increasing processing temperature of MAF [43-44], [79]. Table 3 summarizes the altered properties of various steel alloys during MAF based on processing conditions, materials used, strain applied, final grain size achieved, and the resulting properties.

Table 3: Tabulation of different steels processed, strain applied, refined grains and properties evolved.

Processing	Materials	Equivale-nt Strain	Grain Size	Mechanical Properties	Ref.
MAF at 77K and 300K	Austenitic stainless steel (SUS 316)	6	5-10 nm	UTS-2.1 GPa, Ductility-20%, Hardness-5GPa	[79]
MAF at 500°C and 800°C	Austenitic stainless steel (304 type)	4	0.22 µm at 500°C and 0.69 µm at 800°C	Max. flow stress - about 800 MPa	[44]
MAF at RT	Low carbon steel	2.8	1.2 µm	YS - 850 MPa, UTS - 1115 MPa, Ductility - 7.1%,	[87]
MAF after preheated at 550°C for 45 min	HSLA steel	3.6		YS-814 MPa, UTS-817Mpa, Ductility-14.62%, Toughness-7.78J	[88]
MAF after preheated at 500°C for 50 min.	AISI 1016 steel	7.2	0.6 µm	UTS - 695 MPa, Ductility - 10%, Hardness - 277 Hv	[89]
MAF after preheated at 500 °C and holding for 50 min.	HSLA steel	3.6	0.6 µm	YS - 380 MPa, UTS – 813± 25 MPa, Ductility - 12± 0.2%, Hardness - 274± 7.5 Hv	[90]
MAF at 500°C	Plain low carbon	1.3	0.5 µm	YS – 409±23.3 MPa, UTS – 791± 7.2 MPa, Ductility - 12± 2.43%, Hardness - 253 Hv	[91]
MAF at 600°C	316L stainless steel	4.2	0.86 µm	UTS – 1000±65 MPa Ductility - 14%, Hardness – 334 Hv	[92]
MAF at 500°C	AISI 1024 steel	3.6	0.5 µm	U.T.S - 800 MPa, Ductility - 12%, Hardness - 253 Hv, Wear resistance is not improved	[93]
MAF at 973K in air	AISI201 stainless steel	12	5 µm	True YS around 800 MPa, UTS around 830 MPa	[94]
MAF at temperature between 500°C and 700°C	S304H austenitic stainless steel	3.5	0.1 µm	At 500°C, UTS-810 MPa At 700°C, UTS-490 MPa	[95]

2.3.5 Effect of strain rate

A typical dynamic recrystallization phenomenon generally occurs in a continuous and homogeneous manner during MAF [33]. In a polycrystalline material, various constraints are imposed by the continuity of the grain boundary, which causes a complex strain behaviour at the grain boundary due to the accumulation of strain in each pass in all directions [80]. This results in an increase in the dislocation density on the grain boundaries. The amount of grain boundaries is increased because of the large plastic strain during forging, and the grains become finer. The change in strain path associated with MAF and its higher deformation rates can significantly influence the microstructure development in all temperature ranges. In this case, the high density of the preserved sub-boundaries can effectively absorb the dislocations during straining, leading to a gradual increase in the misorientation of sub-boundaries and transformation of low angle boundaries into high angle boundaries [92], [96]. When the strain rate jumps, additional slip systems get activated by the increased flow stress, which results in rotations of the individual crystallites towards achieving stable orientations in the deformations [97]. Lichtenfeld et al. [98] have studied how strain rate impacts the stress-strain behaviour of austenitic stainless steels. They have found that as the strain rate is increased, the ultimate tensile strength of the material also is increased. In compositions with carbide precipitates, with increasing strain rate, the strain hardening rate decreases because more κ-carbides are sheared by dislocations during deformation at higher strain rates, which causes a reduction in the hindrance to dislocation slip [99].

Increasing the strain rate during MAF leads to a reduction in flow stress due to thermal softening in the deformed volume [100]. Therefore, optimizing the process parameters like strain, strain rate, and temperature is crucial for achieving an ultrafine-grained microstructure through MAF. On straining in each pass, the flow stress rises and produces

a hardening effect because a highly dense dislocation configuration arises, which acts as a barrier to dislocation glide, resulting in an appreciable hardening behaviour [28], [72]. When MAF on Fe-Mn-Al-C low-density steel is carried out, a hardening will be seen in after each pass. So, there is a chance that ductility will decrease with improvement in strength in the subsequent passes. However, with the accurate combination of the austenitic phase of 20-30Mn-8-11Al-0.7-1.2C, 80% elongation could be achieved.

2.3.6 Effect of temperature

The cDRX is occurred during deformation under high strain, producing fine grains at lower temperatures. It may also arise from the fact that decreasing the deformation temperature slows down the grain boundary mobility. At relatively low temperatures, dynamic restoration through long-distance migration of grain boundaries may be hindered. Therefore, an alternative softening way, in which the dislocations are reorganized to form the deformation-induced low angle boundaries and then gradually transformed towards high angle boundaries, might come into operation[101-102]. At higher temperatures, dislocation substructures are annihilated due to the greater ease of dynamic recovery, and precipitate particles dissolve more readily in the matrix. As a result, the number of grains containing MSBs decreases at elevated temperatures, making it more difficult to form ultrafine grains [103]. Conversely, at lower temperatures, finely dispersed particles restrict dislocation rearrangement, leading to the stabilization of the substructure as well as the rapid formation of MSBs and ultrafine grains [79]. At relatively lower temperatures, with austenite decomposing, cDRX of ferrite and the formation of inter-granular k-carbide are responsible for significant softening. At high deformation temperatures where austenite is a dominant phase, dynamic recrystallization is the restoration mechanism [21].

In high-strength materials such as steel, MAF is likely to be performed at temperatures close to the recrystallization range (between 600°C and 700°C) [43-44]. This temperature

range is selected for the forging process because it enhances ductility and helps prevent the formation of undesirable martensite. However, more MAF passes are necessary for grain refinement and improved strength. An alternative approach is to execute MAF under warm temperature conditions. However, the substance should be quite ductile. Akbarian et al. conducted MAF on high-manganese TWIP steel at room temperature, increasing the yield strength from 209.69 MPa and ultimate tensile strength from 430 MPa to 941 MPa and 1079 MPa, respectively, while reducing ductility from 50% to 10%. MAF processes are used by Nakao and Miura [79] to strengthen austenitic steel at both ambient and cryogenic temperatures. They examined steel with ductility of over 100% prior to MAF, but after MAF, it dropped to 20%, with a strength reaching over 2 GPa. Kim et al. [104] confirm that the elongation decreases sharply after one cycle of MAF, but later, it is found that the total elongation does not depend on the number of cycles. This independence is primarily brought on by minor changes in the average geometrically necessary dislocation density due to the dynamic recovery throughout the specimen. According to Sharath et al. [105], the MAF process can potentially improve the material's strength and ductility by promoting the emergence of a finer grain structure when carried out at lower temperatures. Therefore, optimizing the process parameters is crucial to achieving an ultrafine-grained microstructure by MAF.

2.3.7 Use of finite element method in multiaxial forging

As stated in the above sections, strain, strain rate and temperature variation during MAF affect the flow stress in the deformed volume. Therefore, optimizing the process parameters such as strain, strain rate, and temperature is crucial to achieving an ultrafine-grained microstructure by MAF. According to the research done by Zhu et al., fine grains start to form near the specimen's centre during the initial MAF passes [106]. Then, an X-shaped zone with a fine-grained structure emerges in the subsequent passes. The centre of the

specimen gets refined at initial passes, and with increasing strain, the refined zone spreads towards the surface. The refinement at the centre reaches a saturated value for the imposed strain of 6. Thereafter, the surface continuously gets refined beyond strain of 6 up to 12. The accumulated strain is increased with the number of passes, and the distribution of accumulated stain becomes more uniform with a higher number of passes. It is crucial to understand that the mechanical properties of a material are directly influenced by the changes that occur in its microstructure during the process. However, these changes are predominantly regulated by the distribution of equivalent strain within the material. Therefore, understanding the equivalent plastic strain distribution during this forging process has become of prime importance. By understanding the strain distribution, one can alter the deforming parameters to obtain efficient and better-quality results. However, conducting experiments to detail the effect of every process parameter is expensive and time-consuming.

Through the FEM, the critical process parameters can be optimized at a reduced time. FEM is a helpful tool for simulating engineering systems with an expensive experimental setup and a lengthy process to resolve complex issues like MAF that would be challenging to resolve otherwise [47]. Furthermore, when choosing the ideal design scenario, researchers frequently use physical or phenomenological constitutive models that offer insightful information on the underlying mechanisms governing the deformation process of the material. MAF deformation is a complex phenomenon incorporating many mechanisms that function at the micro and atomic scales.

The layer removal method is commonly used to measure residual stress through the thickness of a sample. However, techniques like electro-polishing or machining, which are used in this method, can unintentionally relieve residual stress, posing challenges to accurate measurements [107]. FE modelling has been used to predict residual stress

distribution during forging, with a focus on incorporating initial strain hardening and microstructure evolution [108]. This approach has been applied to various aspects of the forging process, including deformation behaviour and microstructure evolution [109], quench-induced distortions [110], and the optimization of forging parameters to control residual stresses [111]. These studies collectively demonstrate the effectiveness of FEM in simulating and predicting the complex phenomena involved in forging processes. Residual stress conditions in MAF processes are highly dependent on various input parameters and boundary conditions, making them sensitive to experimental approaches. The numerical approach, on the other hand, can reduce the experimental costs and efforts significantly and therefore, FEM plays a crucial role in predicting and evaluating residual stresses in forging processes.

2.4 Residual stress

2.4.1 Definition and classification of residual stresses

Residual stresses represent self-equilibrating internal stresses inherently present in manufactured components, existing independently of external forces and constraints [112]. Residual stress arises due to misfit between two regions. They are categorized by macro stresses and micro stresses [113]. The residual stresses can be grouped into three types:

Type I: Macro residual stress that develops in the body of a component over long distance which is in a scale larger than the grain size of the material. Macro residual stress arises due to shot peening, differential cold deformation, bending, welding etc.

Type II: Micro residual stress that varies on the scale of an individual grain. Low level microscopic residual stresses that vary between grains or intergranular stresses are due to variation in elastic and thermal properties of differently oriented neighbouring grains, but high level stresses arises due to multiple phases or phase transformations.

Type III: Micro residual stresses that exist within a grain in atomic scale, essentially as a result of coherency strain at interfaces, the presence of dislocations and other crystalline defects.

2.4.2 Causes of residual stress

Residual stresses are commonly generated during manufacturing processes that involve material deformation, heat treatment, machining, or any operations that alter the shape or properties of a material. These stresses can originate from various sources and may be present in the unprocessed raw material, introduced during manufacturing, or arise from in-service loading. The origins of residual stresses can be classified as follows [114]:

- differential plastic flow
- differential cooling rates
- phase transformations with volume changes etc.

For example, tensile residual stresses in a component or structural element are generally detrimental, as they can contribute to and often cause fatigue failure and stress-corrosion cracking. Conversely, compressive residual stresses in the sub-surface layers of a material, induced by various means, are typically beneficial. They help prevent the initiation and propagation of fatigue cracks and enhance wear and corrosion resistance.

2.4.3 Different measurement techniques

The residual stresses in materials can be found using a variety of techniques, including layer removal, X-ray and neutron diffraction, hole drilling, and more [114-115]. Techniques for measuring Type I residual stresses (excluding techniques such as diffraction, in which selectively sample grains oriented for diffraction) can be classified as destructive, semi-destructive, or non-destructive. Destructive and semi-destructive techniques, also known as mechanical methods, infer the original stress from the

displacement caused by completely or partially relieving the stress through material removal. These methods rely on measuring the deformations that occur due to the release of residual stresses when material is removed from the specimen. The principal destructive and semi-destructive techniques for measuring residual stresses in structural members include sectioning, contour, hole-drilling, ring-core, and deep-hole methods. Non-destructive methods encompass X-ray or neutron diffraction, ultrasonic methods, and magnetic methods. These techniques typically measure parameters related to stress and are becoming increasingly important for assessing fatigue-related damage. This is crucial for the periodic inspection of structural components such as bridges, aircraft structures, and offshore platforms to prevent significant damage or failure. After studying the residual stress measuring methods from literatures [113], [116-117], several methods are summarized and compared in Table 4.

Table 4: Different methods of residual stress measurement.

Methods	Hole-drilling method	Stripping method
Principle	Measure the strain released by drilling a small hole and calculate stress with equations based on elastic mechanics	Establish the relationship between the removal depth and deformation and calculate the initial stress in workpiece based on elasticity theory
Minimum analysis interval (Depth)	1.2 times of hole diameter	Integral workpiece thickness
Applicable object	Isotropic elastic materials	Hard film materials
Advantage	High measurement accuracy, theoretical maturity	Realizable measurement of residual stress along depth direction
Limitations	Semi destructive testing, complex operation and slow detection speed	Completely destructive testing with low efficiency

Methods	Ring-core method	Contour method	Crack compliance method
Principle	Measure the strain released by drilling a small hole or a ring and calculate stress with equations based on elastic mechanics	Reverse the stress from deformation according to the Bueckner's superposition principle.	Calculate the strain according to superposition principle by introducing cracks with increasing depth on the surface of specimens.
Minimum analysis interval (Depth)	5 mm	Density of test lattices and grid of FEM	1–100 mm
Applicable object	Measurement of residual stress at large depths	Severe variation of internal residual stress	Suitable for aluminium alloy material
Advantage	Large depth measurement range, high accuracy	Large variations in depth direction can be measured	Feasible measurement of residual stress along depth direction
Limitations	Special strain gauges and equipment are needed	Research theory is immature, additional stress is introduced	The measurement accuracy of the method is sensitive to the size of the workpiece

Methods	XRD	Neutron diffraction	Ultrasonic method
Principle	Calculate the stress by Bragg equation according to the diffraction angle through different incident light angles	Measure the strain in three orthogonal directions by Bragg equation	Measure the residual stress according to the acoustic birefringence
Minimum analysis interval (Depth)	20 μm	500 μm	0.5–150 mm
Applicable object	Isotropic elastic crystal materials	Composite and heterogeneous materials	Mainly metallic materials
Advantage	Non-destructive, high accuracy	Non-destructive, strong penetration	High efficiency

Limitations	Can only measure residual stress on the surface	The instrument is expensive, and the detection speed is slow	Imperfect theory, low measurement accuracy

Methods	Raman spectroscopy method	Magnetic method	Nanoindentation technique
Principle	Calculate the stress according to proportional relationship between stress and relative Raman frequency shift in the crystal	Measure internal stress according to the change in the magnetism of a ferromagnetic material	Calculate the residual stress state based on the Hertz contact theory in contact elastic-mechanics
Minimum analysis interval (Depth)	Transverse: 0.5 μm Depth: 2 μm	BN: 0.03–0.2 mm; MAE: 1–2 cm	0.5 mm
Applicable object	Crystalline & composites materials	Ferromagnetic materials	Thin film materials
Advantage	Microstructures can be measured	High efficiency, strong penetration	Easy and fast detection
Limitations	Precision is susceptible to environmental impact	Workpieces need to be magnetized	Imperfect theory

2.4.4 Residual stress measurement by X-ray diffraction

XRD is a widely used non-destructive method for residual stress measurement. This method works exceptionally well for measuring macroscopic stresses under different loading scenarios, offering a unique chance for the thorough study of deformation mechanisms and changes in internal stress in polycrystalline materials. The stress tensor, averaged over the measurement volume, is assumed to produce a linear distribution of d vs. $\sin^2\psi$ in order to calculate stress from the strain data that has been recorded. This linearity manifests when there is no detectable in-depth stress gradient inside the material

depth. However, significant non-linearities can appear in cold-formed polycrystalline materials, as evidenced by oscillating patterns in the d vs. $\sin^2\psi$ plots. Shear stresses are present in these situations normal to the specimen surface, which explains the elliptical trajectory of the d vs $\sin^2\psi$ distribution[118-119].

2.4.5 Residual stresses during multiaxial forging

When metal is forged in bulk deformation, discrete plastic strain changes occur simultaneously in different regions, which lead to the generation of an internal stress distribution [46]. The formation of high strain-induced grain boundaries in very fine grains leads to a non-equilibrium state and the development of a long-range stress field [120]. The inhomogeneous material flow generates residual stress, and the workpiece is characterized by dissimilar material properties. A material with a fixed yield point experiences changes in its yield strength due to residual stresses, acting as a pre-stress condition [121]. In MAF, the close die walls restrict the flow of the plastic material and subject the specimen to triaxial stress. This triaxial stress induces simple shear, leading to the production of ultrafine-grained materials [71]. Chi et al. have investigated the effect of MAF in Al-Zn-Mg-Cu and found that post-deformation heat treatment reduces residual stress, which increases ductility [122]. Nazari et al., on the other hand, have shown that annealing has the reverse impact and it increases residual stress. Also, increasing the number of confined grooves pressing passes decreases the residual stress [123]. They as well have noted that the residual stress on the surface is compressive in character and changes to tensile stress as it approaches the thickness. The amount of residual stress in materials and components is often overestimated, although it can have a significant impact on the mechanical properties of metallic components in both positive and negative ways. Compressive residual stresses commonly confer performance advantages relative to their tensile

counterparts by mitigating crack propagation, consequently enhancing fatigue and fracture behaviour [124-126].

The residual stress within the closed-die MAF is higher than that of the open-die MAF when subjected to an equivalent degree of working. This is because closed die material has greater susceptibility to introduce additional strain within its interior for a specified working ratio per pass [127]. Moazam and Honarpisheh have found that the residual stress created during quenching reduces as MAF passes increase. After two passes, the internal stress becomes more consistent and eased [128]. Noda et al. have further noticed that a rise in equivalent strain is associated with a fall in residual stress; nevertheless, an increase in residual stress is observed above an equivalent strain of 2.4 [129]. While the residual stress distribution has been extensively studied in cold and hot forming processes like extrusion, wire drawing, and rolling, the assessment of the magnitude and distribution of residual stresses throughout the volume in multiaxially forged materials has been relatively less explored until now. Also, if these complex residual stress distributions during MAF are not understood properly, they will impede its application. Previous studies have primarily focused on exploring normal residual stress components, both experimentally and numerically mostly for two-dimensional geometries. Nevertheless, the comprehensive determination of all normal and shear residual stresses remains unexplored for MAF components.

2.5 Constitutive models

An ideal plasticity model for metals should ideally capture key material properties, including strain-rate dependence, temperature dependence, and the effects of strain and strain-rate history, as well as work-hardening or strain-hardening behaviour (both isotropic and anisotropic). However, fully characterizing all these phenomena in one model is a highly complex, if not impossible, task. To make the modelling process more manageable,

certain assumptions must be introduced based on the specific requirements of the application. Several physically and phenomenologically based models have been developed for use in computational mechanics (Table 5). The four widely used constitutive models are: the Johnson-Cook model [130], Zerilli-Armstrong model [131] , Bodner-Partom model [132], and Khan-Huang model [133]. These models are chosen because they have a comparable number of material constants and are relatively straight forward to implement in computational procedures. Models like the Mechanical Threshold Stress model, which have a significantly larger number of material constants or pose computational challenges, are less commonly used in investigations.

Table 5: Comparison of the major characteristics of physically based constitutive models.

Year	Model	Strain rate	Main Features
1975	Bodner and Parton [132]	10-3 to 100 s^{-1}	• Based upon separation of the total deformation rate into elastic and plastic components • Incorporates strain hardening effects through a plastic work term • Assumes a dependency on J2 invariant • No temperature effects
1980	Steinberg and Guinan [134]	10^5 s^{-1}	• Incorporates temperature effects, • Considers the effect of shock pressure • Based on equivalent plastic strain
1987	Zerilli-Armstrong [131]	$4x10^3$ s^{-1}	• Considers temperature effects • Considers grain size • Based on dislocation mechanics • Considers thermal activation
1988	Mechanical threshold stress[135]	10^{-4} to 10^4 s^{-1}	• Incorporates temperature effects • Based on thermal activation • Based on dislocation density as state variable
1983	Johnson and Cook [130]	Up to 10^4 s^{-1}	• Purely empirical model • Considers the effect of temperature • Considers strain rate effects
1992	Khan and Huang [133]	10^{-5} to 10^4 s^{-1}	• Does not include temperature effects

			• Based upon separation of the total deformation rate into elastic and plastic components • Assumes a dependency on J2 invariant
2009	Khan, Liang and Farrokh [136]	10^{-4} to 10^{3} s^{-1}	• Derived from KHL method • Includes temperature effects • Considers grain size
2003	Kocks and Mecking [137]	10^{2} to 10^{4} s^{-1}	• Based on dislocation density • Considers thermal activation • Considers flow stress at 0 K
2005	Molinari & Ravichandran[138]	10^{-3} to $8.5x10^{4}$ s^{-1}	• Based on a characteristic length scale of the microstructure • Considers temperature effects • Considers grain size
2008	Lin, Chen and Zhong [139]	$5x10$ s^{-1}	• Defines flow stress in terms of the Zener-Hollomon parameter
2009	Huang et al. [140]	10^{-5} to 10^{6} s^{-1}	• Dislocation mechanics • Thermal activation • Temperature

2.5.1 Plasticity models during the deformation of Fe-Mn-Al-C alloy steels

Previously, many researchers have developed material model for Fe-Mn-Al-C alloy steels based on Arrhenius equation or parameters in equation to describe the plastic flow characteristics at different hot working regimes [141-143]. They accounted the role of dynamic recrystallization and activation energy in the ease of deformation at higher working temperature. However, the reports on the evolution of activation energy and dynamic recrystallization at low temperature deformation are so rare. Wan et al. constructed physical phenomena (self-diffusion coefficient) based constitutive model for Fe-Mn-Al-C alloys steel for flow behaviour in hot deformation regimes [144]. Wang et al. modelled rate and temperature dependent plasticity model based on dislocation density and twinning phenomena and showed the deviation in term of the average relative error between the calculated and experimental values as 5.6% [145]. Recently, crystal plasticity finite element method is also used for polycrystalline material as another potentially powerful

method to study deformation twinning and the interaction of twin and slip at the microstructure level [18]. However, the effect of strain rate and temperature was absent in these models. So far, different phenomenological models and physical models were explored to investigate the deformation behaviour of Fe-Mn-Al-C alloys steel. The actual crystal plasticity which takes place during deformation (such as micro band induced plasticity, twinning, deformation induced martensite, grain refinement) is so complex that a simplified model based on the one principle is difficult to account all these effects in one equation.

Now a days, experimental investigations have developed the J-C empirical relationship to understand metallurgical processes. The J-C constitutive model [146] has been successfully applied to various carbon steel alloys [147-148], dual phase steel [149-150], aluminum alloys [151], nickel [152] and can be adopted for ductile material such as austenitic low-density steel. Hasan et al. have determined the J-C model parameters for high manganese steel (11% and 14%Mn) through uniaxial tensile tests and conducted FE simulation to analyse plasticity and ductility due to dynamic loading [153]. Wang et al. formed the J-C constitutive model to describe the strain hardening and strain rate effect in high specific strength light weight steel [154]. This material model is extensively used in FE analysis platform (such as ABAQUS explicit, ANSYS explicit, Ls Dyna, Autodyne) to generalize the laboratories data and applied to industrial practices. It is efficient and cost-effective tool for correctly investigating the plastic deformation processes.

Because of some interesting inherent properties of low-density steel, this material has emerged as an alternative to replace conventional steel and a better material choice for vehicle body design. However, the lack of theoretical and computational studies on material behaviour in different loading conditions slows down the applicability of various manufacturing processes. A significant amount of research work is required to control the

loading conditions for product design corresponding to ductility and to predict the actual stresses developed during deformation.

Now a days, to replicate same material behaviour of experiments (such as machining, metal forming, dynamic loading) accurately, optimization algorithms are being adopted for constitutive models to give best overall fit [148], [155-156]. GA is one of the most popular algorithms opted by practitioners to solve multi objective optimization problems in design control system [157-159]. This technique is used to solve engineering optimization problems based on natural selection. Initially, it selects the random population of individual solution under predefined constrained, then performs exchange of information to create a superior offspring for the next iteration. Over successive iterations, the population of individuals toward optimal solution is reached that suits the initial environmental conditions.

Looking at the futuristic application of low-density steel in numerous areas, it appears that both theoretical and experimental investigations are required for austenite-based Fe–Mn–Al–C low-density steel in order to determine the flow stress during deformation. Even though, in the open literature, several research works are available for metal forming of low-density steels, only a few researchers have derived the J–C constitutive model for Fe–Mn–Al–C low-density steel at intermediate strain rates and elevated temperatures [154]. In automobile industry, the forming of automobile parts occurs at intermediate strain rate level or above, and therefore, it needs a comprehensive understanding of strain rate-based deformation behaviour.

2.5. 2 Constitutive modelling of multiaxial forging

Choosing the ideal design scenario, researchers frequently use physical or phenomenological constitutive models that offer insightful information on the underlying mechanisms governing the deformation process of the material. MAF deformation is a

complex phenomenon incorporating many mechanisms that function at the micro and atomic scales. For a physical model, it is frequently necessary to apply advanced characterization methods like SEM, TEM, and EBSD to fully comprehend the underlying micro or atomistic mechanisms [47], [160]. The information gained from these instruments aids in developing physics-based models, which are essential in precisely forecasting and optimizing the deformation process. Phenomenological constitutive models establish the relationship between the imposed process parameters (strain, temperature, and strain rate) and the material response, usually the flow stress [47-48]. But these models do not include the microstructural features like grain size or dislocation density at every stage of MAF for a realistic representation of the material behaviour.

SPD induces strain hardening in the material by forming dislocations within the crystal lattice structure, which increases the strength of the material by making it more difficult to deform further. Wing et al. [161] and Caruso et al. [162] have used the modified J-C phenomenological model incorporated with the effect of grain refinement during dynamic loading to predict the correct flow stress after each pass of MAF. Furthermore, the effect of dislocation density has been incorporated in the J-C model to predict the flow stress pattern and shape of the deformed body by Youan et al. [163] in machining-induced deformation problem and Rohan et al. [164] in cold spray process. These models aid in creating better processing methods for improved material performance and offer insightful information on the underlying mechanisms governing the deformation process of the material. To the best of the author's knowledge, in MAF till today, there is no such J-C model and the FEM based studies available where the microstructure features such as dislocation density, grain size together are included in the J-C model to predict the flow stress.

2.6 Research gaps

1. Through proper control of chemical composition and thermomechanical processes in low-density steel, grain refinement is limited only up to 10 - 20 μm.
2. No published works have been available on strengthening by grain refinement through MAF on Fe-Mn-Al-C based low-density steel.
3. Empirical models have been formulated to study the plastic behavior during severe plastic deformation, but a material model with effect of grain size and dislocation density for low-density steel has not been studied.
4. FEA of MAF on conventional steels are available, but no simulation work has been performed to predict yield strength and residual stresses during MAF of low-density steel.

2.7 Objectives

The objectives of the present thesis are to develop fine-grained high strength low-density austenitic and duplex steels by multiaxial forging technique and the prediction of yield strength as well as residual stress using Johnson-Cook and modified Johnson-Cook models.

The objectives are aimed:

1. to design of composition to get low-density in austenitic/duplex steel.
2. to optimize the process parameters to prepare designed alloy by induction melting and casting to get defect free material.
3. to design die and deform selected alloys by MAF to get refined structure for achieving high strength.
4. to characterize steels for microstructure, mechanical properties and residual stress.

5. to evaluate the J-C parameters for coarse grained as well as multiaxially forged steels to predict yield strength and flow stress through FEM.
6. to evaluate and predict the residual stress distribution throughout the volume in coarse grained as well as multiaxially forged low-density steel.